Chalcogen Stabilized *bis*-Hydridoborate Complexes of Cobalt: Analogues of Tetracyclo[4.3.0.0^{2,4}.0^{3,5}]nonane

Benson Joseph,[a] Suman Gomosta,[a] Rini Prakash,[a] Thierry Roisnel,[b] Ashwini K. Phukan*[c] Sundargopal Ghosh*[a]

[a] Dr. B. Joseph, S. Gomosta, Dr. R. Prakash, Prof. S. Ghosh
Department of Chemistry
Indian Institute of Technology Madras
Chennai 600036, India
E-mail: sghosh@iitm.ac.in
[b] Dr. T. Roisnel
Institut des Sciences Chimiques de Rennes
Université de Rennes, CNRS,
UMR 6226, F-35000 Rennes, France.
[c] Prof. A. K. Phukan
Department of Chemical Sciences
Tezpur University
Napaam 784028, Assam, India.
E-mail: ashwini@tezu.ernet.in

Supporting information for this article is given via a link at the end of the document.

Abstract: Treatment of Li[BH$_3$ER] (E = Se or Te, R = Ph; E = S, R = CH$_2$Ph) with [Cp*CoCl]$_2$ led to the formation of hydridoborate complexes, [{CoCp*Ph}{Cp*Co}{μ-EPh}{μ-κ^2-E,H–EBH$_3$}], **1a** and **1b** (**1a**: E = Se; **1b**: E = Te) and a *bis*-hydridoborate species [Cp*Co{μ-κ^2-Se,H–SeBH$_3$}]$_2$, **2**. All the complexes, **1a**, **1b** and **2** are stabilised by β-agostic type interaction in which **1b** represents a novel bimetallic borate complex with a rare B-Te bond. QTAIM analysis furnished direct proof for the existence of a shared and dative B-chalcogen and Co-chalcogen interactions, respectively. In parallel to the formation of the hydridoborate complexes, the reactions also yielded tetracyclic species, [Cp*Co{κ^3-E,H,H–E(BH$_2$)$_2$–C$_5$Me$_5$H$_3$}], **3a** and **3b** (**3a**: E = Se and **3b**: E = S), wherein the bridgehead boron atoms are surrounded by one chalcogen, one cobalt and two carbon atoms of a cyclopentane ring. Molecules **3a** and **3b** are best described as the structural mimic of tetracyclo[4.3.0.0^{2,4}.0^{3,5}]nonane having identical structure and similar valence electron counts.

Introduction

Since the isolation of Zeise's salt, K[PtCl$_3$(C$_2$H$_4$)].H$_2$O,[1] transition metal complexes containing carbon-based ligands have been extensively explored. As a result organometallic chemistry of the d-block, is very well established.[2] In contrast, the chemistry of complexes with boron or a combination of boron and carbon, have picked up pace only in the past few decades.[3] Unlike carbon, the structural chemistry of boron exhibits a more complex electronic structure which is associated with its typical electron-deficient nature.[3] However, the pioneering work by Stock, Lipscomb, Brown and Shore on polyhedral boranes[3] alongside the discovery of isolobal analogy[4] and electron counting rules,[5] presented an entirely new domain of structural chemistry that offered unique structures and novel bonding archetypes. As a result, several classic organometallic species that define fundamental structural and bonding paradigms, are found to be mimicked by isoelectronic transition metal borane complexes.[6] For example, diborane(4) complex, [{Cp*Mo(CO)$_2$}$_2${μ-η^2:η^2–B$_2$H$_4$}] can be considered as a true valence isoelectronic analogue of Mo and W-alkyne complexes, [{CpMo(CO)$_2$}$_2${μ-η^2:η^2–C$_2$H$_2$}] and [{CpW(CO)$_2$}$_2${μ-η^2:η^2–C$_2$R$_2$}] (R = C$_6$H$_4$Me or Me) respectively.[6a,6b] In addition, several other organometallic species are also mimicked by metallaboranes. For example, [(PR$_3$)ClPdC$_3$H$_5$] vs. [(PR$_3$)$_2$PdB$_3$H$_7$],[6c] [CpCo(C$_4$H$_4$)] vs. [CpCo(B$_4$H$_8$)],[6d] [Cp$_2$Fe] vs. [CpFe(B$_5$H$_{10}$)],[6e] and [Cp*Ru(C$_8$H$_6$)RuCp*] vs. [Cp*Ru(B$_8$H$_{14}$)RuCp*].[6f]

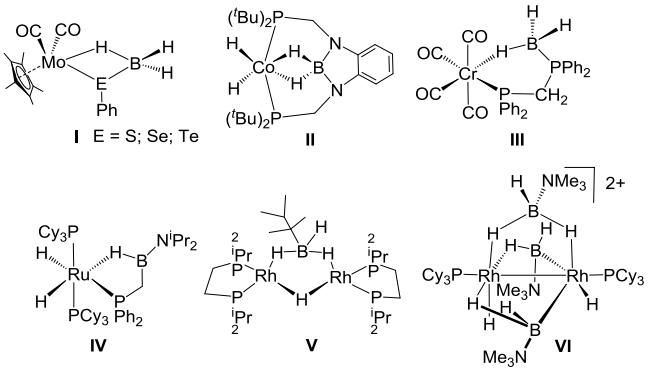

Scheme 1. Mono and bimetallic agostic borane/borate complexes of transition metals

Apart from structural interest, complexes containing boron-centered ligand with boron-metal linkage via hydrogen, have attracted considerable interest due to their applications in catalysis.[7] As a result, reactivity of various σ-borane[8] and hydrido-,

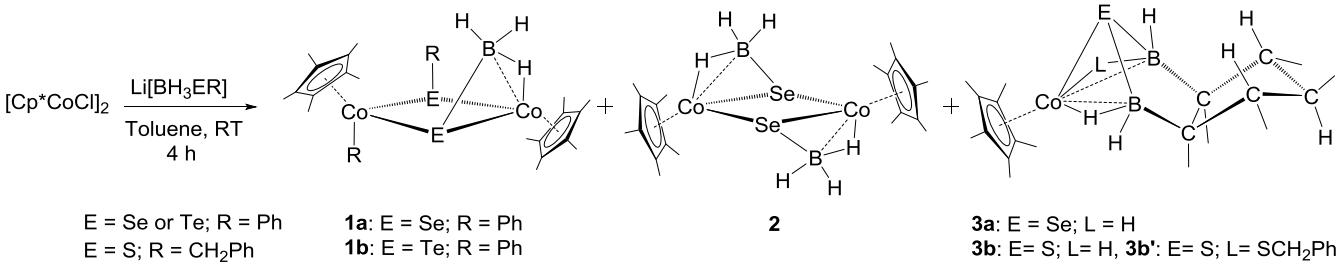

Scheme 2. Synthesis of hydridoborate borate complexes **1a**, **1b**, **2**, **3a**, **3b** and **3b'**

borate[9] complexes have been extensively studied. In a similar context, weak B-H···M interaction in pyrazolyl borate or similar heterocyclic scorpionate borate ligands have also attracted significant attention.[10] As shown in Scheme 1, the agostic type of secondary interaction observed in hydridoborate species (**I** and **II**)[11,12] is similar to that of borane-Lewis base adduct complexes (**III** and **IV**).[13] The donor atoms, which are bonded to metal, are generally limited to N, P and S in all these cases and to the best of our information, the effect of the heavier group 16 elements on agostic type B-H···M interaction, other than species **III**, is less studied. Understanding this effect is important as one can tune the reactivity of these species by altering the activation of the B-H bond. In addition, the sigma and agostic complexes reported till date are mostly restricted to monometallic species, with a few exceptions (**V** and **VI**).[14]

Results and Discussion

Reactivity of $[Cp^*CoCl]_2$ with $Li[BH_3ER]$ (E = Se or Te, R = Ph; E = S, R = CH_2Ph).

Existence of several structural varieties, shown in Scheme 1, motivated us to develop new methods for the synthesis of chalcogen stabilized borate species supported by agostic type interaction. Recently, we have shown that borate species $Li[BH_3EPh]$ and $Na[BH_3(SCHS)]$ can be utilized for the synthesis of different types of Mo and Ru-agostic type complexes.[11a,15] As a result, the utilization of these species with other transition metals became of interest. Therefore, we explored the reactivity of $[Cp^*CoCl]_2$ with $Li[BH_3EPh]$ (E = Se and Te) that led to the formation of bimetallic hydridoborate species, [{CoCp*Ph}{Cp*Co}{μ-EPh}{μ-κ^2–E,H-EBH_3}], **1a** and **1b** (**1a**: E = Se; **1b**: E = Te) and *bis*-hydridoborate complex $[Cp^*Co\{\mu\text{-}\kappa^2\text{-}Se,H\text{–}SeBH_3\}]_2$, **2** (Scheme 2). All these species feature a four-membered metallaheterocycle (Co_2E_2) comprising of agostic type interaction. To the best of our knowledge, **1b** is the first structurally characterized borate complex featuring a B-Te bond.[16]

The new borate complexes **1a** and **1b** were isolated as violet and green crystals respectively, which were characterized by ^1H, ^{11}B, and ^{13}C NMR and IR spectroscopies along with single-crystal X-ray crystallography. The mass spectra of **1a** and **1b** showed intense isotopic distribution pattern at *m/z* 716.0440 and 814.9902 corresponding to $[M]^+$ and $[M+3H]^+$ respectively. The ^{11}B NMR spectra of them showed one upfield chemical shift at δ = -16.9 and -21.5 ppm for **1a** and **1b** respectively that suggest the presence of borate species. The ^1H NMR spectra of **1a** and **1b** show the presence of two types of terminal-BH and a single Co-H-B proton. The {^1H–^{11}B} HSQC experiment clearly linked these protons with the single boron. Although all the spectroscopic data along with mass spectrometric data suggest **1a** and **1b** are of similar structure, in order to confirm the spectroscopic assignments and to determine the solid-state structure of **1a** and **1b**, the X-ray structure analysis was undertaken. Based on the X-ray structural data, shown in Figure 1, it appears that the Co-B bond distances are significantly shorter as compared to typical sigma or hydridoborate complexes of Co.[17] The B–Te bond distance of 2.229(4) Å is comparable with the previously reported B-Te single bond distances.[16] Two of the Co(III) centres are linked by chalcogeneto ligands $[EPh]^-$ and $[EBH_3]^{2-}$ (E = Se or Te). Further, the Co···Co distances of 3.5065(7) Å and 3.7676(8) Å for **1a** and **1b** respectively, clearly suggest the absence of any metal–metal bond making them coordinatively saturated 18e species. Addition of phenyl group into one of the Co centers is interesting. We believe that the Ph fragment has been generated by the cleavage of E-C bond of in-situ generated $Li[BH_3ER]$, which is very unstable in nature. The metal might also have played an important role in activating the E-Ph bond in the reagent.[18]

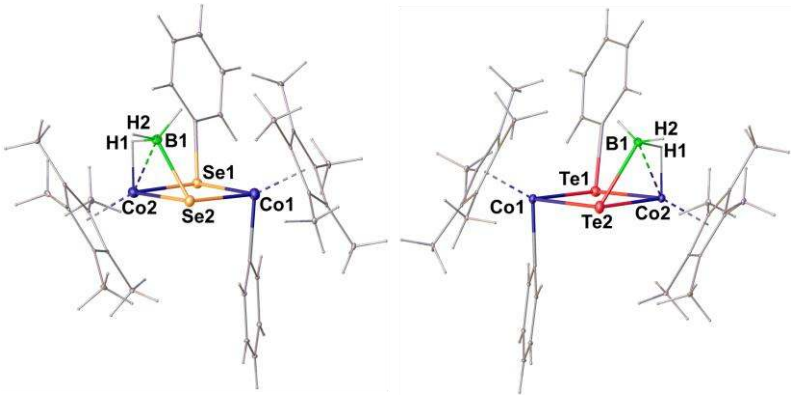

Figure 1 Molecular structures and labelling diagrams for **1a** (left) and **1b** (right). Selected bond lengths (Å) and angles (°) for **1a**: Co2-Se1 2.3546(6), Co2-B1 2.295(4), B1-Se2 2.017(4), Co2-H1 1.55(3), B1-H1 1.30(3), Co1···Co2 3.5065(7); B1-H1-Co2 107(2), For **1b**: Co2-Te2 2.5231(5), Co1-Te2 2.5371(5), Co2-B1 2.327(4), B1-Te2 2.229(4), Co2-H1 1.59(4), B1-H1 1.13(2), Co1···Co2 3.7676(8).

Compound **2** was isolated as brown solid in 49% yield. The ^{11}B NMR spectrum shows one sharp signal at δ = -15.9 ppm and the ^{1}H NMR displays one upfield chemical shift at δ = -12.01 ppm. The mass spectrometric data shows an ionised peak at *m/z* 574.9974. The solid-state X-ray structure of **2**, shown in Figure 2, indicates a highly symmetric bimetallic *bis*-hydridoborate species crystallized in $P2_1/n$ space group as a centrosymmetric molecule. Both the metal centers are connected by two $[SeBH_3]^{2-}$ moieties similar to that of **1a** and **1b**. In **2**, the BH_3 units are associated with cobalt through an η^1-HB coordination mode. The B-H_b distance of 1.37(4) Å is slightly longer and the Co-H_b (1.53(4) Å) and Co-B (2.262(4) Å) distances are slightly shorter as compared to **1a** and **1b**. The B–Se bond length of 2.038(3) Å is within the range of Lewis base-stabilized boron organoselenide species, for example, 1,2-diselenatoorthocarboranes (B–Se: 1.975(4)-2.065(5) Å),[19a-b] and CAAC-supported cyanoboron bis(selenide), [(CAAC)B(CN)(SePh)$_2$] (B–Se: 2.109(7), 2.056(8) Å).[19c] Alternatively, **2** can also be viewed as the borane analogue of $[(Cp^*Co)_2(\mu\text{-}S)_2(\kappa\text{-}S)_2]$ or $[(CpCo)(E_2C_6H_4)]_2$ (E = S or Se),[20] in which the S or (EC_6H_4) (E = S or Se) units are replaced by BH_3 moiety. The calculated HOMO-LUMO gap ($\Delta E_{H\text{-}L}$) measured for **2** and $[(Cp^*Co)_2(\mu\text{-}S)_2(\kappa\text{-}S)_2]$ signify higher thermodynamic stability for **2** ($\Delta E_{H\text{-}L}$ = 4.38 eV and 3.55 eV for **2** and $[(Cp^*Co)_2(\mu\text{-}S)_2(\kappa\text{-}S)_2]$ respectively).

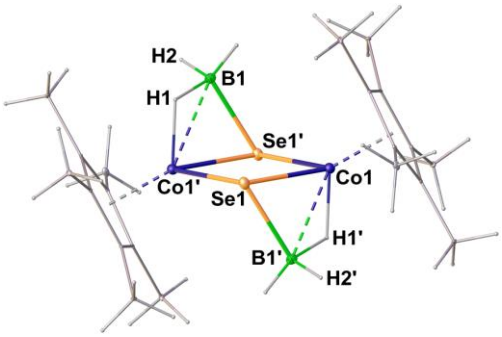

Figure 2. Molecular structure and labelling diagram for **2**. Selected bond lengths (Å) and angles (°): Co1-Se1 2.3628(5), Co1'-Se1 2.3716(5), Co1-B1 2.262(4), B1-Se1 2.038(3), Co-H1 1.53(4), B1-H1 1.37(4), Co1···Co1' 3.5020(6); Se1-Co1-Se1'84.59(15).

One of the interesting features of **1a**, **1b** and **2** is the presence of a nearly planar Co_2E_2 metallaheterocyclic ring. Compound **2** displays a perfectly planar ring with a torsion angle of 0°, while the rings of **1a** and **1b** are slightly deviated from planarity with a maximum torsional angle of 2.13° and 1.52° respectively. The sum of the internal angle measured for **1a** and **1b** is 359.97° and for **2** is 360°. Although the $\{Co_2E_2\}$ (E = S, Se or Te) core is known for $[Co(PMe_3)_3E]_2$, the angle of deviation from 90° is more prominent there, generating diamond type structures.[21]

To have further insight into the bonding of these hydridoborate species, especially the agostic type B-H···Co interaction, DFT based computations were performed on these molecules and most of the computed geometrical parameters are in good agreement with the observed values (Table S1). Natural bond orbital (NBO) analysis shows extensive charge transfer from chalcogen to boron as well as cobalt centres. This is evident from an increase in the natural valence population or charges (more negative) on B and Co and decreases on chalcogen atoms (Table S2). The relatively lower computed $\Delta E_{H\text{-}L}$ value for **1b** as compared to **1a** and **2** may be attributed to the presence of a significantly longer Co-Co bond in **1b.**

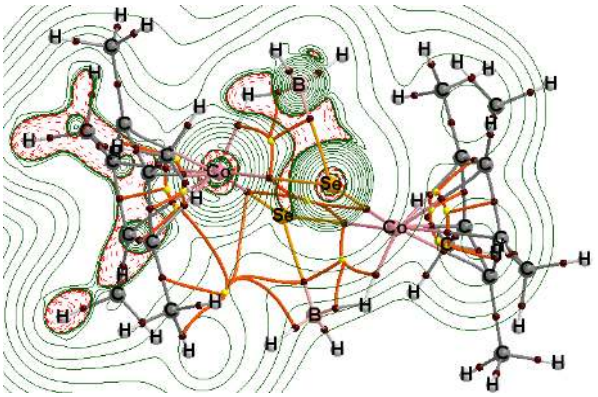

Figure 3. Contour line diagram of the Laplacian of electron density in the Co–Se–B plane of **2**. Solid green lines indicate charge depletion [$\nabla^2\rho$(r)>0] and dashed maroon lines indicate charge concentration [$\nabla^2\rho$(r)<0]. Dark maroon and yellow spheres denote bond critical points (bcp) and ring critical points (rcp) respectively.

The nature of chalcogen–boron interaction in **1a**, **1b** and **2** is probed by QTAIM analysis. Figure 3 shows the contour map of the Laplacian of electron density $\nabla^2\rho$(r) for **2** along the Co-Se-B plane that exhibits continuous region of charge concentration formed by the valence shell charge concentration (VSCC) zone of boron and selenium.[22] The chalcogen–boron interaction has more covalent character in **1a** and **2** than that of **1b**. This has been signified not only by higher values of electron density (ρ_b) at the bond critical point (bcp) but also by larger and higher negative values of Laplacian of the electron density ($\nabla^2\rho$) and energy density, H(r) at bcp (Tables S3-S5). The nature and the extent of Co-H and B-H interactions are similar in **1a**, **1b** and **2**. In contrast to the covalent or shared nature of boron-chalcogen interactions, the Co-Se/Te interactions are dative in nature as illustrated by comparatively lower electron density (ρ_b) at the bcp and positive values of Laplacian of the electron density ($\nabla^2\rho$).[23] On the other hand, the agostic B-H interactions have high degree of covalent character as ascertained from higher values of ρ_b as well as negative values of H(r). These values are essentially similar for **1a**, **1b** and **2** (Tables S3-S5).

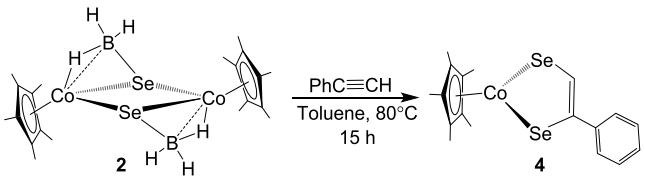

Scheme 3. Reactivity of **2** with phenylacetylene

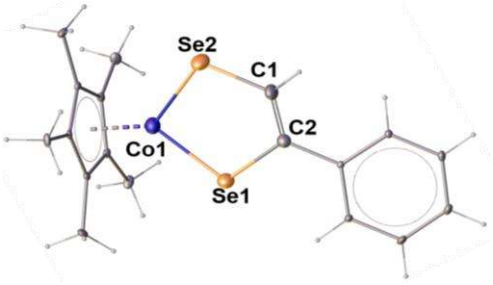

Figure 4. Molecular structure and labelling diagram for **4**. Selected bond lengths (Å) and angles (°): Co1-Se2 2.2265(6), Se1-Co1 2.2317(5), Se2-C1 1.865(3), Se1-C2 1.888(3), C1-C2 1.334(5); Co1-Se2-C1 103.03(1), Se2-C1-C2 122.8(3), Se1-Co1-Se2 92.29(2).

Sigma/agostic complexes are known for the hydroboration of alkynes.[24,25] Hartwig *et al*. has reported the reactivity of $[Cp_2Ti(HBcat)_2]$ with terminal and internal alkynes that resulted in the formation of hydroborated product in major yield along with the formation of a metallacycle.[24a] Later, he has shown the utility of them as efficient catalysts for the hydroboration of vinyl arenes.[24b] Recently, Muhoro *et al*. also used the same complex as a catalyst for the hydroboration of ketones and aldehydes.[24c] We have also explored the reactivity of various hydridoborate and borane complexes with alkynes that led to the formation of hydroborated products.[25] As a result, we were interested to investigate the reactivity of these Co-hydridoborate complexes for authenticating its efficacy as hydroborating agent. Hence, we performed the reactivity of **2** with phenylacetylene at thermolytic condition that led to the formation of a green compound, **4** in 20% yield (Scheme 3). Multinuclear NMR and X-ray crystallographic analysis revealed **4** as cobalt-selenium metallaheterocycle, [Cp*Co{κ^2-Se,Se–Se_2C_2HPh}], which was spectroscopically characterised by Morley's group.[26] The solid-state structure of **4** is shown in Figure 4. Compound **4** might have formed through the borane displacement from **2**, which was confirmed by trapping the free borane as $BH_3{\cdot}PCy_3$ adduct.

In parallel to the formation of hydridoborate species, the reaction of $[Cp^*CoCl]_2$ and $Li[BH_3(SePh)]$ also yielded **3a**, isolated as red crystals, which is characterised by ^1H, ^{11}B, and ^{13}C NMR and IR spectroscopies and by single-crystal X-ray crystallography. The ^{11}B NMR shows a peak at δ = -0.01 which is downfield shifted as compared to **1a**, **1b**, and **2**. The ^1H NMR spectrum indicates the presence of Co-H-B protons. Although the ^{11}B and ^1H chemical shifts have a similar trend to those of **1a**, **1b**, and **2**, the ^1H NMR of **3a** shows some additional peaks in the aliphatic region (δ = 0.95-1.30 ppm) and the ^{13}C NMR shows resonances in the region of δ = 11.1-53.1 ppm.

In order to have a clear picture of **3a**, the X-ray structure analysis was undertaken. The solid-state X-ray structure of **3a**, shown in Figure 5(a), depicts the composition as [Cp*Co(κ^3-Se,H,H-$Se(BH_2)_2$–$C_5Me_5H_3$}], having a unique tetracyclic *bis*-hydridoborate structure. In an attempt to isolate the sulphur analogue of **3a**, the reaction was carried out with $Li[BH_3SPh]$ that led to decomposition. However, the similar reaction with $Li[BH_3SBn]$, (Bn = CH_2Ph) yielded **3b** and **3b'**.[27] **3b** shows similar spectroscopic data as that of **3a** indicative of analogous structure. Indeed, the X-ray diffraction analysis confirmed **3b** (Figure 5(b)) as the sulphur analogue of **3a**. The S and the Se atoms lie above the Co-B-B and B-B-C-C planes. Compound **3b'** is analogous to **3a** and **3b**, the only difference between the structures of **3b** and **3b'** is the replacement of one of the bridging hydrogens by SCH_2Ph unit in the later (Figure 6). Like **2**, both **3a** and **3b** have agostic type interactions along with additional co-ordination from chalcogen to metal. In general, borate complexes are stabilised by heterocyclic scorpionate-type frameworks.[10] However, in case of **3a**, **3b** and **3b'**, the hydridoborate groups are stabilised by cyclo-pentane ring. The boron chalcogen distances (**3a**: B-S 1.915(3) Å; **3b**: B-Se 2.0611(9) Å) are similar to those observed in trichalcogeno-1,3-diborolanes with sp^3 boron atoms.[16d,19c,28] The C-C and B-C bond distances of **3a** and **3b** are slightly elongated as compared to the corresponding C-C and B-C single bond distances.[19]

The solid-state X-ray structures of **3a** and **3b** may be considered as the analogue of tetracyclo[4.3.0.$0^{2,4}$.$0^{3,5}$]nonane (Figure 5(c)).[29] In general, mimicking of organometallic complexes by metallaboranes take place when the borane moiety substitutes the analogous organic counterpart. Some of the examples known in the literature typically range from metal-alkene to dinuclear ruthenium–pentalene π-complexes.[6] Similarly, complexes having boron containing heterocyclic π ligands, such as, bora/dibora-benzene and borole/diborole etc. are also analogues to corresponding metal-arene complexes.[30-32] However, there are only a few cases known with the metal-boron

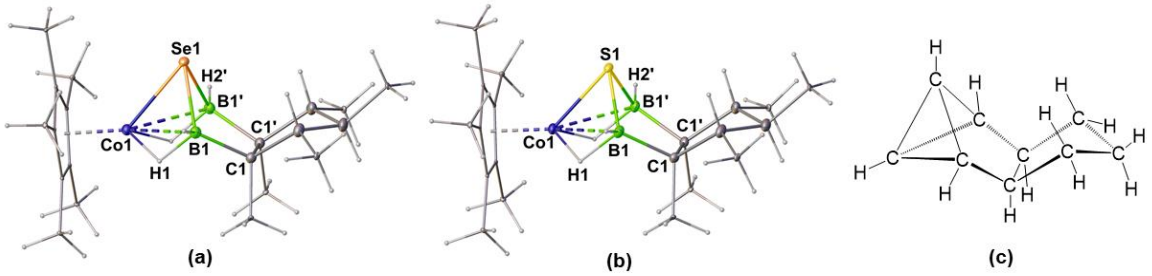

Figure 5. Molecular structure and labelling diagram for a) **3a** and b) **3b**. Selected bond lengths (Å) and angles (°) for **3a**: Co1-Se1 2.3109(5), Co1-B1 2.3426(19), B1-Se1 2.0611(19), Co1-H1 1.550(19), B1-H1 1.278(19), B1-C1 1.613(3), C1-C1' 1.595(2); B1-H1-Co1 112, B1-Se1-Co1 64.50(5), B1-Se1-B1' 80.29(11). For **3b**; Co1-S1 2.1918(9), Co1-B1 2.316(2), B1-S1 1.915(3), Co1-H1 1.54(2), B1-H1 1.33(3), B1-C1 1.612(3), C1-C1' 1.591(4); B1-H1-Co1 108, B1-S1-Co1 68.28(3), B1-S1-B1' 85.22(16); c) Schematic representation of tetracyclic [4.3.0.$0^{2,4}$.$0^{3,5}$] nonane.[29]

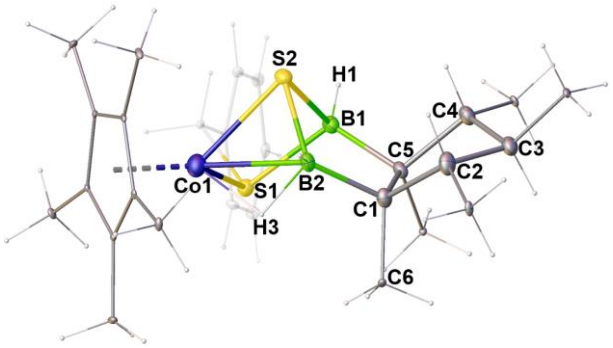

Figure 6. Molecular structure and labelling diagram for **3b'**. Selected bond lengths (Å) and angles (°):Co1-S2 2.2498(9), Co1-S1 2.2492(9), Co1-B2 2.277(4), S1-B1 1.975(4), S2-B2 1.902(4), Co1-H3 1.56(4), B2-H3 1.38(4); Co1-S1-B1 88.47(11), B1-S2 Co1 88.74(11), Co1-H3-B2 101(2), B2-S2-B1 88.06(16).

framework which is analogues to hydrocarbons. For instance, clusters $[\{CpM\}_4B_4H_4]$ (M = Ni or Co) are analogous to parent cubane, C_8H_8.[33] Interestingly, the mimicking of entire tetracyclic nonane framework of **3a** and **3b** is very unusual and considered to be the perfect example that shows the bridge between hydrocarbon and metal borane/borate complexes. The C_5 ring in one part of the tetracyclic nonane and **3a** or **3b** is somewhat similar, whereas the bridgehead carbon atoms of the other part have been replaced by two boron atoms connected through sulphur and cobalt bridges. As shown in Scheme S4, the total valence electron (tve) count of 58 for **3a** or **3b** matches well with tetracyclo[4.3.0.$0^{2,4}$.$0^{3,5}$]nonane (tve = 48). Thus, one can describe these species as true structural mimic of tetracyclo[4.3.0.$0^{2,4}$.$0^{3,5}$]nonane. In addition, from the cluster point of view, if one considers the cyclic alkane part as the ligand on boron, $[(Cp^*CoE)(BH_2R)_2]$ unit in **3a** and **3b** can be viewed as an *arachno*-butterfly with 7 sep.

Although the syntheses and structures of saturated boron-chalcogen heterocycles are known in the literature,[16b-d,19] their utilization as ligands is not explored. Hence, structures of **3a**, **3b** and **3b'** need attention due to the presence of 1-chalcogeno-3,4-dicarba-2,5-diborolane ligand fragment connected to cobalt in trihapto mode. Though, we don't have any direct evidence for the formation of these species, we believe that they might have generated *in situ* while reducing the Cp* ligand by chalcogenated borohydride that subsequently reacted with the metal fragment. A similar reduction and activation of the Cp ligand are reported in the literature.[34] Thus, it is reasonable to assume that the reduction of Cp* ligand might have been initiated by the chalcogenoborate reagent followed by the formation of complexes **3a** or **3b.**

DFT calculation at the same level of theory indicates that the charge transfer from the chalcogen atoms mostly takes place to the metal, albeit lower than those observed for **1** and **2** (Table S6). The computed $\Delta E_{H\text{-}L}$ values for **3a** and **3b** are higher than those computed for **1a**, **1b** and **2** (Tables S2 and S6) which may be attributed to the presence of relatively shorter cobalt-chalcogen bonds in the former. The $\Delta E_{H\text{-}L}$ value of the tellurium analogue of **3** is found to be 3.92 eV which is 0.6-0.8 eV lower as compared to **3a** and **3b**. This is also supported by the presence of weaker Co-Te (WBI = 0.579) and Te-B (WBI = 0.711) interactions as compared to stronger Co-Se (WBI = 0.731) and Se-B (WBI = 0.925) interactions. These weaker interactions possibly account for the instability of the tellurium analogue of **3a** or **3b** which may be the reason that several of our attempts to isolate the tellurium analogue failed.

The nature of chalcogen–boron interaction in **3a** and **3b** has also been probed by QTAIM analysis (Figure 7). The Laplacian plot illustrates not only the continuous region of charge concentration between boron and sulphur but also exhibits diffusion or polarization of the VSCC zone of sulphur towards cobalt. The chalcogen-boron interaction has significant covalent character as evident from high and negative values of $\nabla^2\rho$ and H(r) at the bcp (Tables S7-S8). Unlike **1a**, **1b** and **2**, the Co-S/Se interactions in **3a** and **3b** are dative in nature, which is represented by comparatively lower electron density (ρ_b) at the bcp as well as positive values of $\nabla^2\rho$. However, the nature and extent of B-H agostic type interactions in **3a**, **3b** and **3b'** are similar to those in **1a**, **1b** and **2**, i.e., the B-H interactions are significantly covalent in nature.

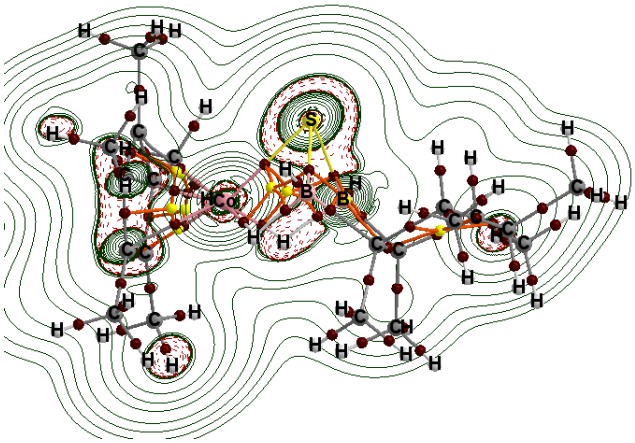

Figure 7. Contour line diagram of the Laplacian of electron density in the Co–S–B plane of **3b**. Solid green lines indicate charge depletion [$\nabla^2\rho(r)>0$] and dashed maroon lines indicate charge concentration [$\nabla^2\rho(r)<0$]. Dark maroon and yellow spheres denote bond critical points (bcp) and ring critical points (rcp) respectively.

Conclusions

In conclusion, an efficient route for the synthesis of novel cobalt hydridoborate complexes using arylchalcogenoborate, $Li[BH_3ER]$ (E = Se or Te, R = Ph; E = S, R = CH_2Ph) and $[Cp^*CoCl]_2$ has been established. Complexes **1a**, **1b** and **2** represent unique bimetallic cobalt heterocyclic systems, which are stabilised by β-agostic type interaction. Most importantly, distinctive tetracyclic species, **3a**-**b** have been isolated and structurally characterized, which may be considered as a true structural mimic of tetracyclo[4.3.0.$0^{2,4}$.$0^{3,5}$]nonane. These molecules exemplify a rare class of hydrocarbon mimic by metal borate complex. In addition, AIM analysis establishes that in all the species, the boron-chalcogen interaction has significant covalent character

while the Co-Se/Te interactions are largely dative in nature. In an effort to verify the potentiality of these complexes, especially the *bis*-hydridoborate species, for the hydroboration of alkynes, it yielded cobaltaselenacycles by borane displacement. Further exploration of the chemistry employing these complexes are underway.

Experimental Section

All the syntheses were carried out under an argon atmosphere with standard Schlenk line and glove box techniques. Compounds $[Cp^*CoCl]_2$[35] and $Li[BH_3ER]$ (E = S, Se or Te, R = Ph; E = S, R = CH_2Ph)[11a] were prepared according to literature methods. Thin-layer chromatography was carried out on 250 mm aluminium supported silica gel TLC plates. NMR spectra were recorded in a 500 MHz Bruker FT-NMR spectrometer. Chemical shifts are referenced to (residual) solvent signals ($^1H/^{13}C\{^1H\}$; $CDCl_3$: δ = 7.26/77.16 ppm, $^1H/^{13}C\{^1H\}$; C_6D_6: δ = 7.16 /128.06 ppm). Infrared spectra were obtained on a Jasco FT/IR–1400 spectrometer in dichloromethane solvent. The Electrospray mass (ESI-MS) spectra were measured in micromass Q-TofmicroTM instrument and Thermo Scientific LTQ XL Linear Ion Trap Mass Spectrometer.

Syntheses of 1a, 2 and 3a: A suspension of $[Cp^*CoCl]_2$ (0.100 g, 0.22 mmol) in 8 mL toluene at -78 ° C was charged dropwise with freshly prepared solution of $Li[BH_3SePh]$ in THF (10 mL, 0.44 mmol) over 15 min and kept under constant stirring for 4h at room temperature. The colour of the reaction mixture changed from brown to black gradually during course of the reaction. The solvent was evaporated in vacuum; residue was extracted into hexane/CH_2Cl_2 (90:10 v/v) and passed through Celite. After the removal of the solvent from the filtrate, the residue was subjected to chromatographic workup using silica-gel TLC plates. Elution with hexane/CH_2Cl_2 (70:30 v/v) yielded violet [{CoCp*Ph}{Cp*Co}{μ-SePh}{μ-κ^2-Se,H–$SeBH_3$}], **1a** (0.026 g, 16%, R_f = 0.58), brown $[Cp^*Co\{\mu\text{-}\kappa^2\text{-}Se,H\text{–}SeBH_3\}]_2$,**2** (0.062 g, 49%, R_f = 0.48) and red $[Cp^*Co\{\kappa^3\text{-}Se,H,H\text{–}Se(BH_2)_2\text{–}C_5Me_5H_3\}]$,**3a** (0.027 g, 14%, R_f = 0.79)

1a: ESI-MS (ESI^+) calcd for $C_{32}H_{43}BSe_2Co_2$ $[M]^+$*m/z* 716.0465, found 716.0440; $^{11}B\{^1H\}$ NMR (160 MHz, $CDCl_3$, 22 °C): δ = -16.9 ppm (s, 1B); $^1H\{^{11}B\}$ NMR (500 MHz, $CDCl_3$, 22 °C): δ = 8.08 (s, 1H, $C_6\underline{H}_5$), 7.92 (d, *J* = 7.7 Hz, 3H, $C_6\underline{H}_5$), 7.21-7.18 (m, 2H, $C_6\underline{H}_5$), 7.09 (t, *J* = 7.6 Hz, 3H, $C_6\underline{H}_5$), 6.96 (t, *J* = 7.1 Hz, 1H, $C_6\underline{H}_5$), 2.12 (s, 1H, B$\underline{H}_t$), 1.96 (s, 1H, B$\underline{H}_t$), 1.18 (s, 15H, $C_5\underline{Me}_5$), 0.97 (s, 15H, $C_5\underline{Me}_5$), -9.86 ppm (br, 1H, Co-$\underline{H}$-B); $^{13}C\{^1H\}$ NMR (125 MHz, $CDCl_3$, 22ºC): δ = 163.1 (s, $\underline{C}$-Co), 145.1, 136.2, 127.6, 126.6, 126.0, 125.1, 121.8 (s, $\underline{C}_6H_5$), 91.9, 90.3 (s, $\underline{C}_5Me_5$), 9.6, 9.2 ppm (s, $C_5\underline{Me}_5$); IR (CH_2Cl_2): $\tilde{\nu}$ = 2400 (BH_t).

2: ESI-MS (ESI^+) calcd for $C_{20}H_{35}B_2Co_2Se_2$ $[M\text{-}H]^+$*m/z* 574.9932, found 574.9974; $^{11}B\{^1H\}$ NMR (160 MHz, C_6D_6, 22 °C): δ = -15.9 ppm (s, 1B); $^1H\{^{11}B\}$ NMR (500 MHz, C_6D_6, 22 °C): δ = 2.60 (s, 2H, B$\underline{H}_t$), 2.34 (d, 2H, B$\underline{H}_t$),1.50 (s, 30H, $C_5\underline{Me}_5$), -12.01 (d, 2H, Co-$\underline{H}$-B); $^{13}C\{^1H\}$ NMR (125 MHz, $CDCl_3$, 22ºC): δ = 91.4 (s, $\underline{C}_5Me_5$), 10.0 ppm (s, $C_5\underline{Me}_5$); IR (CH_2Cl_2): $\tilde{\nu}$ = 2462, 2400 (BH_t).

3a: ESI-MS (ESI^-) calcd for $C_{20}H_{37}B_2CoSe$ $[M]^-$*m/z* 438.15, found 438.22; $^{11}B\{^1H\}$ NMR (160 MHz, C_6D_6, 22 °C): δ = -0.0 ppm (s, 1B); ^1H NMR (500 MHz, C_6D_6, 22 °C): δ = 2.57 (br, 2H, B$\underline{H}_t$), 1.45 (s, 15H, $C_5\underline{Me}_5$), 1.30 (br, 3H, C$\underline{H}$), 1.14 (d, 6H, C$\underline{H}_3$), 0.96 (d, 3H, C$\underline{H}_3$), 0.95 (s, 6H, C$\underline{H}_3$), -15.25 (br, 2H, Co-$\underline{H}$-B); $^{13}C\{^1H\}$ NMR (125 MHz, $CDCl_3$, 22ºC): δ = 93.9 (s, $\underline{C}_5Me_5$), 53.1 (s, $\underline{C}$HMe), 47.9 (s, $\underline{C}$HMe), 19.3 (s, CH$\underline{Me}$), 16.5 (s, CH$\underline{Me}$), 13.5 (s, CH$\underline{Me}$), 11.1 ppm (s, $C_5\underline{Me}_5$); IR (CH_2Cl_2): $\tilde{\nu}$ = 2420 (BH_t).

Synthesis of 1b: A suspension of $[Cp^*CoCl]_2$ (0.100 g, 0.22 mmol) in 8 mL toluene at -78 °C was charged dropwise with freshly prepared solution of $Li[BH_3TePh]$ in THF (10 mL, 0.44 mmol) over 15 min and kept under constant stirring for 4h at room temperature. The colour of the reaction mixture changed from brown to dark green gradually during course of the reaction. The solvent was evaporated in vacuum; residue was extracted into hexane/CH_2Cl_2 (90:10 v/v) and passed through Celite. After the removal of the solvent from the filtrate, the residue was subjected to chromatographic workup using silica-gel TLC plates. Elution with hexane/CH_2Cl_2 (70:30 v/v) yielded green, [{CoCp*Ph}{Cp*Co}{μ-TePh}{μ-κ^2-E,Te–$TeBH_3$}],**1b** (0.098 g, 55%, R_f = 0.52).

1b: ESI-MS (ESI^+) calcd for $C_{32}H_{46}BTe_2Co_2$ $[M+3H]^+$*m/z* 815.0455, found 814.9902; $^{11}B\{^1H\}$ NMR (160 MHz, $CDCl_3$, 22 °C): δ = -21.5 (s, 1B) ppm; ^1H NMR (500 MHz, $CDCl_3$, 22 °C): δ = 8.08 (d, *J* = 7.3 Hz, 2H, $C_6\underline{H}_5$), 7.91 (d, *J* = 7.5 Hz, 2H, $C_6\underline{H}_5$), 7.30 (t, *J* = 7.4 Hz, 1H, $C_6\underline{H}_5$), 7.12 (t, *J* = 7.5 Hz, 2H, $C_6\underline{H}_5$), 7.00 (t, *J* = 7.3 Hz, 2H, $C_6\underline{H}_5$), 6.91 (t, *J* = 7.1 Hz, 1H, $C_6\underline{H}_5$), 3.97 (br, 1H, B$\underline{H}_t$), 2.10 (br, 1H, B$\underline{H}_t$), 1.45 (s, 15H, $C_5\underline{Me}_5$), 1.24 (s, 15H, $C_5\underline{Me}_5$), -10.96 ppm (br, 1H, Co-$\underline{H}$-B); $^{13}C\{^1H\}$ NMR (125 MHz, $CDCl_3$, 22ºC): δ = 160.8 (s, $\underline{C}$-Co), 148.0, 139.0, 137.7, 129.4, 127.9, 126.1, 121.6 (s, $\underline{C}_6H_5$), 91.6, 90.1 (s, $\underline{C}_5Me_5$), 10.7, 10.1 ppm (s, $C_5\underline{Me}_5$); IR (CH_2Cl_2): $\tilde{\nu}$ = 2404 (BH_t).

Synthesis of 3b and 3b': A suspension of $[Cp^*CoCl]_2$(0.100 g, 0.22 mmol) in 8 mL toluene at -78 °C was charged dropwise with freshly prepared solution of $Li[BH_3S(CH_2Ph)]$ in THF (10 mL, 0.44 mmol) over 15 min and kept under constant stirring for 4h at room temperature. The colour of the reaction mixture changed from brown to black gradually during course of the reaction. The solvent was evaporated in vacuum; residue was extracted into hexane/CH_2Cl_2 (90:10 v/v) and passed through Celite. After the removal of the solvent from the filtrate, the residue was subjected to chromatographic workup using silica-gel TLC plates. Elution with hexane/CH_2Cl_2 (70:30 v/v) yielded orange$[Cp^*Co\{\kappa^3\text{-}S,H,H\text{–}S(BH_2)_2\text{–}C_5Me_5H_3\}]$, **3b** (0.048 g, 28%, R_f = 0.8), purple, $[Cp^*Co\{\kappa^3\text{-}S,H,S\text{–}S(BH_2)(BHSBn)\text{–}C_5Me_5H_3\}]$, **3b'** (0.011 g, 5%, R_f = 0.68) and blue, known $[(Cp^*Co)_2(BHS)_2]$ (0.027 g, 26%).[36]

3b: HR-MS (ESI^-) calcd for $C_{20}H_{37}B_2CoS$ $[M]^-$*m/z* 390.21, found 390.30; $^{11}B\{^1H\}$ NMR (160 MHz, C_6D_6, 22 °C): δ = -1.8 ppm (s, 1B); ^1H NMR (500 MHz, C_6D_6, 22 °C): δ = 1.99 (br, 2H, B$\underline{H}_t$), 1.48 (m, 2H, C$\underline{H}$Me), 1.43 (s, 15H, $C_5\underline{Me}_5$), 1.27 (m, 1H, C$\underline{H}$Me) 1.14 (d, *J* = 6.9 Hz, 6H, CH$\underline{Me}$), 0.96 (d, *J* = 6.4 Hz, 3H, CH$\underline{Me}$), 0.94 (s, 6H, CH$\underline{Me}$), -15.75 (br, 1H, Co-$\underline{H}$-B); $^{13}C\{^1H\}$ NMR (125 MHz, C_6D_6, 22ºC): δ = 94.6 (s, $\underline{C}_5Me_5$), 53.6 (s, $\underline{C}$HMe), 48.7 (s, $\underline{C}$HMe), 20.1 (*s,* CH$\underline{Me}$), 17.3 (*s,* CH$\underline{Me}$), 14.6 (*s,* CH$\underline{Me}$), 10.8 ppm (s, $C_5\underline{Me}_5$); IR (CH_2Cl_2): $\tilde{\nu}$ = 2415 (BH_t) cm^{-1}.

3b': HR-MS (ESI^+) calcd for $C_{27}H_{44}B_2CoS_2$ $[M+H]^+$*m/z* 513.2413, found 513.2379; $^{11}B\{^1H\}$ NMR (160 MHz, C_6D_6, 22 °C): δ = 11.2 (s, 1B), 2.8 ppm (s, 1B); ^1H NMR (500 MHz, C_6D_6, 22 °C): δ =7.39 (d, *J* = 7.6 Hz, 2H, $C_6\underline{H}_5$), 7.13 (s, 2H, $C_6\underline{H}_5$), 7.05 (s, 1H, $C_6\underline{H}_5$), 3.59 (dd, *J* = 51.1, 12.0 Hz, 2H, $C\underline{H}_2C_6H_5$), 1.79 (br, 1H, B$\underline{H}_t$), 1.47 (s, 1H, C$\underline{H}$Me), 1.37 (s, 1H, C$\underline{H}$Me), 1.33 (s, 3H, CH$\underline{Me}$), 1.29 (s, 15H, $C_5\underline{Me}_5$), 1.27 (s, 3H, CH$\underline{Me}$), 1.16 (br, 1H, B$\underline{H}_t$), 1.06 (d, *J* = 7.2 Hz, 1H, C$\underline{H}$Me), 1.01 (d, *J* = 5.9 Hz, 3H, CH$\underline{Me}$), 0.96 (d, *J* = 6.8 Hz, 3H, CH$\underline{Me}$), 0.55 (s, 3H, CH$\underline{Me}$), -11.25 (br, 1H, Co-$\underline{H}$-B); $^{13}C\{^1H\}$ NMR (125 MHz, $CDCl_3$, 22ºC): δ = 138.6 (s,1C, $\underline{C}_6H_5$-CH_2), 129.1, 128.2, 127.0 (s, $\underline{C}_6H_5$), 92.8 (s, $\underline{C}_5Me_5$), 54.7 (s, S-$\underline{C}H_2$-Ph), 47.5 (s, $\underline{C}$HMe), 43.9 (s, $\underline{C}$HMe), 40.5 (s, $\underline{C}$HMe), 21.3 (s, CH$\underline{Me}$), 16.5 (s, CH$\underline{Me}$), 14.9 (s, CH$\underline{Me}$), 13.9 (s, CH$\underline{Me}$), 13.2 (s, CH$\underline{Me}$), 10.2 ppm (s, $C_5\underline{Me}_5$); IR (CH_2Cl_2): $\tilde{\nu}$ = 2421 (BH_t).

Synthesis of 4: A suspension of **2** (0.050 g, 0.09 mmol) in 8 mL toluene was charged with phenylacetylene (0.018g, 0.18 mmol) kept under constant stirring for 15h at 80 °C temperature. The colour of the reaction mixture changed from brown to dark green gradually during the course of

the reaction. The solvent was evaporated in vacuum; the residue was extracted into hexane/CH_2Cl_2 (90:10 v/v) and passed through Celite. After the removal of the solvent from the filtrate, the residue was subjected to chromatographic workup using silica-gel TLC plates. Elution with hexane/CH_2Cl_2 (70:30 v/v) yielded green, [Cp*Co{κ^2-Se,Se–Se_2C_2HPh}], **4** (0.016 g, 20%),[26, 37] some other low yield compounds could not be isolated.

Computational details: All the molecules were fully optimized with the Gaussian 09[38] program using the meta–GGA M06 exchange correlation functional[39] in conjunction with Def2-TZVP basis set.[40] Frequency calculations were performed at the same level of theory to verify the nature of the stationary state. All structures were identified as ground states as their respective Hessian (matrix of analytically determined second derivative of energy) was real. Natural bonding analyses were performed with the natural bond orbital (NBO) partitioning Scheme[41] as implemented in the Gaussian 09 suite of programs. Dispersion effects were incorporated by using the D3 version of Grimme's dispersion correction coupled with the D3 damping function using the keyword "Empirical Dispersion=GD3" as implemented in Gaussian 09.[42]

X-ray Structure Determination analysis details: Suitable X-ray quality crystals of **1a**-**b**, **2**, **3a**-**b**, **3b'** and **4** were grown by slow evaporation of a hexane-CH_2Cl_2 solution. The crystal data were collected and integrated using a Bruker AXS Kappa APEXII CCD for **1a**, **3a** and **4** and D8 VENTURE Bruker AXS for **1b**, **2**, **3b** and **3b'** with graphite monochromated MoKα (λ = 0.71073 Å) radiation at 150 K (for **1a**, **1b**, **2**, **3b** and **3b'**) and 296(2) K (for **3a** and **4**). The structures were solved by heavy atom methods using SHELXS-97, SHELXT-2014[43] and refined using SHELXL-2014, SHELXL-2017, SHELXL-2018[44]. Hydrogen atoms were located through Fourier map analysis and then refined with the help of the AFIX 2 SHELXL instruction. The molecular structures were drawn using Olex2.[45]. These data can be obtained free of charge from The Cambridge Crystallographic Data Centre via www.ccdc.cam.ac.uk/data_request/cif.

Crystal data for 1a: CCDC 1951417, $C_{32}H_{43}BCo_2Se_2$, M_r = 714.25, Triclinic, space group *P*-1, a = 10.4314(3) Å, b = 14.2851(6) Å, c = 13.6125(5) Å, α = 83.9883 (13)°, β = 83.2778(12)°,γ = 67.1401(11)°, V = 1528.69(7) Å^3, Z = 2, ρ_{calcd} = 1.552 g/cm^3, μ = 3.486 mm^{-1}, F(000) = 724, R_1 = 0.0297, wR_2 = 0.0603, 5368 independent reflections [2θ≤52.6°] and 356 parameters.

Crystal data for 1b: CCDC 1951411, $C_{32}H_{43}BCo_2Te_2$, M_r = 811.53, Triclinic, space group *P*-1, a = 10.5505(12) Å, b = 11.2282(12) Å, c = 14.5991(15) Å, α = 84.354(4)°, β = 87.400(4)°,γ = 64.587(4)°, V = 1554.5(3) Å^3, Z = 2, ρ_{calcd} = 1.734 g/cm^3, μ = 2.926 mm^{-1}, F(000) = 796, R_1 = 0.0278, wR_2 = 0.0635, 7110 independent reflections [2θ≤54.968°] and 353 parameters.

Crystal data for 2: CCDC 1951416, $C_{20}H_{36}B_2Co_2Se_2$, M_r = 573.89, Monoclinic, space group $P2_1/n$, a = 8.1337(10) Å, b = 9.5589(13), c = 15.0561(16) Å, α = 90°, β = 99.661(4)°,γ = 90°, V = 1154.0(2) Å^3, Z = 2, ρ_{calcd}= 1.652 g/cm^3, μ = 4.594 mm^{-1}, F(000) = 576, R_1 = 0.0347, wR_2 = 2632 independent reflections [2θ ≤ 50.484°] and 132 parameters.

Crystal data for 3a: CCDC 19514618, $C_{20}H_{37}B_2CoSe$, M_r= 432.97, Orthorhombic, P_{nma}, a = 21.321(3) Å, b = 12.6368(19) Å, c = 7.9770(13), α = 90°, β = 90°, γ = 90°, V = 2149.3(6) Å^3, Z = 4, ρ_{calcd} = 1.338 g/cm^3, μ = 2.491 mm^{-1}, F(000) = 896, R_1 = 0.0259, wR_2 = 0.0621, 2784 independent reflections [2θ≤50.484°] and 130 parameters.

Crystal data for 3b: CCDC 19514615, $C_{20}H_{37}B_2CoS$, M_r= 390.10, Orthorhombic, P_{nma}, a = 21.168(2) Å, b = 12.8145(15) Å, c = 7.8536(8) Å, α = 90°, β = 90°,γ = 90°, V = 2130.4(4) Å^3, Z = 4, ρ_{calcd} = 1.216 g/cm^3, μ = 0.903 mm^{-1}, F(000) = 840, R_1 = 0.0439, wR_2 = 0.1063, 2538 independent reflections [2θ≤54.964°] and 130 parameters.

Crystal data for 3b': CCDC 19514614, $C_{27}H_{43}B_2CoS_2$, M_r= 512.28, Monolinic, $P2_1/c$, a = 8.3156(10) Å, b = 19.6072(18) Å, c = 16.998(2) Å, α = 90°, β = 99.599(5)°,γ = 90°, V = 2732.7(5) Å^3, Z = 4, ρ_{calcd} = 1.245 g/cm^3, μ = 0.794 mm^{-1}, F(000) = 1096, R_1 = 0.0549, wR_2 = 0.1296, 6191 independent reflections [2θ≤54.996°] and 296 parameters.

Crystal data for4: CCDC 1964166, $C_{18}H_{21}CoSe_2$, M_r= 454.20, Monolinic, $P2_1/c$, a = 15.0177(12) Å, b = 8.7332(7) Å, c = 14.1688(10) Å, α = 90°, β = 106.878(2)°,γ = 90°, V = 1778.2(2) Å^3, Z = 4, ρ_{calcd} = 1.697 g/cm^3, μ = 5.050 mm^{-1}, F(000) = 896.0, R_1 = 0.0324, wR_2 = 0.0595, 3922 independent reflections [2θ≤ 54.268°] and 195 parameters.

Acknowledgements

This work was supported by CEFIPRA (Project No. 5905-1), New Delhi, India. B.J. thanks, UGC and S.G. and R. P. thank IIT Madras for their research fellowships. A.K.P. thanks the Department of Science and Technology (DST-SERB), New Delhi for providing financial assistance in the form of a research project (project no. EMR/2016/005294).

Keywords: cobalt • arylchalcogenoborate • agostic • hydridoborate • metallaheterocycle.

[1] W. C. Zeise, K. Overs, *Dan. Vidensk. Selsk. Forh.* **1825**-**26**, 13.

[2] C. J. Jones, *d- and f-Block Chemistry,* Royal Society of Chemistry: Cambridge, UK, 2001.

[3] a) R. N. Grimes, *Carborane*, 2nd ed.; Elsevier: Amsterdam, 2011; b) C. E. Housecroft, *Boranes and Metalloboranes: Structure, Bonding and Reactivity*, Halsted Press: New York, 1990; c) W. N. Lipscomb, *Boron Hydrides*, Benjamin, New York, 1963; d) F. G. A. Stone, *Adv. Organomet. Chem.* **1990**, *31*, 53-89; e) S. A. Brew, F. G. A. Stone F. G. A. Stone, *Adv. Organomet. Chem.* **1993**, *35*, 135-186; f) T. D. Mcgrath and F. G. A. Stone, *Adv. Organomet. Chem.* **2005**, *53*, 1-40.

[4] R. Hoffmann, *Angew. Chem. Int. Ed. Engl.* **1982**, *21*, 711-724.

[5] a) K. Wade, *Inorg. Nucl. Chem. Lett.* **1972**, *8*, 559-562; b) K. Wade, *Adv. Inorg. Chem. Radiochem.* **1976**, *18*, 1-66; c) D. M. P. Mingos, D. J. Wales, *Introduction to Cluster Chemistry*, Prentice Hall, New York, 1990; d) E. D. Jemmis, M. M. Balakrishnarajan, P. D. Pancharatna, *J. Am. Chem. Soc.* **2001**, *123*, 4313-4323.

[6] a) B. Mondal, R. Bag, S. Ghorai, K. Bakthavachalam, E. D. Jemmis, S. Ghosh, *Angew. Chem. Int. Ed.* **2018**, *57*, 8079-8083; b) J. A. K. Howard, J. C. Jeffery, J. C. V. Laurie, I. Moore, F. G. A. Stone, A. Stringer, *Inorg. Chim. Acta* **1985**, *100*, 23–32; c) L. J. Guggenberger, A. R. Kane, E. L. Muetterties, *J. Am. Chem. Soc.* **1972**, *94*, 5665–5673; d) T. L. Venable, E. Sinn, R. N. Grimes, *J. Chem. Soc. Dalton Trans.* **1984**, 2275-2279; e) R. Weiss, R. N. Grimes, *J. Am. Chem. Soc.* **1977**, *99*, 8087-8088; f) S. Ghosh, B. C. Noll, T. P. Fehlner, *Angew. Chem. Int. Ed.* **2005**, *44,* 6568-6571.

[7] a) G. Alcaraz, S. Sabo-Eitenne, *Coord. Chem. Rev.* **2008**, *252*, 2395-2409; b) K. K. Pandey, *Coord. Chem. Rev.* **2009**, *253*, 37-55.; c) W. H. Harman, J. C. Peters, *J. Am. Chem. Soc.* **2012**, *134*, 5080−5082.

[8] a) C. N. Muhoro, X. He, J. F. Hartwig, *J. Am. Chem. Soc.* **1999**, *121,* 5033-5046; b) M. Shimoi, S.-i. Nagai, M. Ichikawa, Y. Kawano, K. Katoh, M. Uruichi, H. Ogino, *J. Am. Chem. Soc.* **1999**, *121,* 11704-

11712; c) V. M.-Palma, M. Lumbierres, B. Donnadieu, S. Sabo-Etienne, B. Chaudret, *J. Am. Chem. Soc.* **2002**, *124*, 5624-5625; d) T. M. Douglas, A. B. Chaplin, A. S. Weller, X. Yang, M. B. Hall, *J. Am. Chem. Soc.* **2009**, *131*, 15440-15456; e) R. N. Perutz, S. Sabo-Etienne, *Angew. Chem. Int. Ed.* **2007**, *46*, 2578-2592; f) D. Vidovic, D. A. Addy, T. Krämer, J. McGrady, S. Aldridge, *J. Am. Chem. Soc.* **2011**, *133*, 8494-8497; g) M. V. Câmpian, E. Clot, O. Eisenstein, U. Helmstedt, N. Jasim, R. N. Perutz, A. C. Whitwood, D. Williamson, *J. Am. Chem. Soc.* **2008**, *130*, 4375–4385.

[9] a) X. Zheng, J. Huang, Y. Yao, X. Xu, *Chem. Commun.* **2019**, *55*, 9152-9155; b) M. A. Nesbit, D. L. M. Suess, J. C. Peters, *Organometallics* **2015**, *34*, 4741−4752; c) S. Murugesan, B. Stöger, M. Weil, L. F. Veiros, K. Kirchner, *Organometallics* **2015**, *34*, 1364−1372; d) L. Maria, A. Paulo, I. C. Santos, I. Santos, P. Kurz, B. Spingler, R. Alberto, *J. Am. Chem. Soc.* **2006**, *128*, 14590-14598.

[10] a) R. C. da Costa, B. W. Rawe, A. Iannetelli, G. J. Tizzard, S. J. Coles, A. J. Guwy, G. R. Owen, *Inorg. Chem.* **2019**, *58*, 359−367; b) L. R. Kadel, J. R. Bullinger, R. R. Baum, C. E. Moore, D. L. Tierney, D. M. Eichhorn, *Eur. J. Inorg. Chem.* **2016**, 2543–2551; c) A. Caballero, F. G-la Torre, F. A. Jalón, B. R. Manzano, A. M. Rodríguez, S. Trofimenkoc, M. P. Sigalas, *J. Chem. Soc.*, *Dalton Trans.* **2001**, 427–433.

[11] a) R. Ramalakshmi, K. Saha, D. K. Roy, B. Varghese, A. K. Phukan, S. Ghosh, *Chem. Eur. J.* **2015**, *21*, 17191-17195; b) T.-P. Lin, J. C. Peters, *J. Am. Chem. Soc.* **2013**, *135*, 15310-15313; c) G. R. Owen, *Chem. Commun.* **2016**, *52*, 10712-10726; d) J. Brugos, J. A. Cabeza, P. García-Álvarez, E. Pérez-Carreñob, J. F. Van der Maelen, *Dalton Trans.* **2017**, *46*, 4009-4017; e) B. Bera, Y. P. Patil, M. Nethaji, B. R. Jagirdar, *Dalton Trans.* **2011**, *40*, 10592-10597

[12] a) K. Saha, R. Ramalakshmi, S. Gomosta, K. Pathak, V. Dorcet, T. Roisnel, J.-F. Halet, S. Ghosh, *Chem. Eur. J.* **2017**, *23*, 9812-9820; b) M. Zafar, R. Ramalakshmi, K. Pathak, A. Ahmad, T. Roisnel, S. Ghosh, *Chem. Eur. J.* **2019**, *25*, 13537-13546.

[13] a) Y. Gloaguen, G. Alcaraz, A. S. Petit, E. Clot, Y. Coppel, L. Vendier, S. Sabo-Etienne, *J. Am. Chem. Soc.* **2011**, *133*, 17232-17238; b) N. Merle, G. Koicok-Köhn, M. F. Mahon, C. G. Frost, G. D. Ruggerio, A. S. Weller, M. C. Willis, *Dalton Trans.* **2004**, 3883-3892; c) M. Blug, D. Grünstein, G. Alcaraz, S. Sabo-Etienne, X.-F. Le Goff, P. Le Flocha. N. Mézailles, *Chem. Commun.* **2009**, 4432-4434; d) Y. Gloaguen, G. Alcaraz, A-F. Pécharman, E. Clot, L. Vendier, S. Sabo-Etienne, *Angew. Chem. Int. Ed.* **2009**, *48*, 2964-2968; (e) B. Bera, Y. P. Patil, M. Nethaji, B. R. Jagirdar, *Dalton Trans.* **2011**, *40*, 10592-10597.

[14] a) R. T. Baker, D. W. Ovenall, R. L. Harlow, *Organometallics* **1990**, *9*, 3028-3030; b) A. B. Chaplin, A. S. Weller, *Angew. Chem. Int. Ed.* **2010**, *49*, 581-584.

[15] K. Saha, U. Kaur, S. Kar, B. Mondal, B. Joseph, P. K. S. Antharjanam, S. Ghosh, *Inorg. Chem.* **2019,** *58*, 2346-2353.

[16] a) R. Köuster, G. Seidel, W. Schüußler, B. Wrackmeyer, *Chem. Ber.* **1995**, *128*, 87-89; b) H. Braunschweig, P. Constantinidis, T. Dellermann, W. C. Ewing, I. Fischer, M. Hess, F. R. Knight, A. Rempel, C. Schneider, S. Ullrich, A. Vargas, J. D. Woollins, *Angew. Chem. Int. Ed.* **2016**, *55*, 5606-5609; c) S. Liu, M.-A. Légaré, D. Auerhammer, A. Hofmann, H. Braunschweig, *Angew. Chem. Int. Ed.* **2017**, *56*, 15760-15763; d) S. Liu, M.-A. Légaré, A. Hofmann, A. Rempel, S. Hagspiel, H. Braunschweig, *Chem. Sci.* **2019**,*10*, 4662-4666.

[17] a) S. Murugesan, B. Stoger, M. Weil, L. F. Veiros, K. Kirchner, *Organometallics* **2015**, *34*, 1364-1372 and references therein.

[18] M. D. Curtis, S. H. Druker, *J. Am. Chem. Soc.* **1997,** *119*, 1027-1036.

[19] a) B., E. V. Klimkina, W. Milius, *Eur. J. Inorg. Chem.* **2011**, 4481-4492; b) B. Wrackmeyer, E. V. Klimkina, W. Milius, *Polyhedron* **2010**, *29*, 2324-2334; c) D. Auerhammer, M. Arrowsmith, R. D. Dewhurst, T. Kupfer, H. Braunschweig, *Chem. Sci.* **2018**, *9*, 2252-2260.

[20] a) H. Brunner, N. Janietz, W. Meier, G. Sergeson, J. Wachter, T. Zahn, M. L. Ziegler, *Angew. Chem. Int. Ed. Engl.* **1985**, *24*, 1060-1061; b) S. Habe, T. Yamada, T. Nankawa, J. Mizutani, M. Murata, H. Nishihara, *Inorg. Chem.* **2003**, *42*, 1952-1955.

[21] H. -F. Klein, M. Gaß, U. Koch. B. Eisenmann, H. Schäfer, *Z. Naturforsch.* **1988**, *43b*, 830-838.

[22] R. F. W. Bader, *Chem. Rev.***1991**, *91*, 893-928.

[23] The Co-Se/Te interactions do possess some amount of covalent character as manifested by small negative values of energy density, H(r) at bcp (Tables S3-S5).

[24] a) J. F. Hartwig, C. N. Muhoro, X. He, *J. Am. Chem. Soc.* **1996,** *118,* 10936-10937; b) J. F. Hartwig, C. N. Muhoro, *Organometallics* **2000**, *19*, 30-38; c) A. A. Oluyadi, S. Ma, C. N. Muhoro, *Organometallics* **2013**, *32*, 70-78.

[25] a) K. Saha, B. Joseph, R. Ramalakshmi, R. S. Anju, B. Varghese, S. Ghosh, *Chem. Eur. J.* **2016**, *22*, 7871-7878; b) S. Gomosta, K. Saha, U. Kaur, K. Pathak, T. Roisnel, A. K. Phukan, S. Ghosh, *Inorg. Chem.* **2019**, *58*, 9992-9997.

[26] C. P. Morley, R. R. Vaughan, *J. Organomet. Chem.***1993**, *444*, 219-222

[27] Note that the reaction of $[Cp^*CoCl]_2$ with $Li[BH_3S(CH_2Ph)]$ also yielded known $[(Cp^*Co)_2BH)_2S_2]$ in 26% yield.

[28] M. Yalpani, R. Köster, R. Boese, *Eur. J. Inorg. Chem.* **1990**, *123*, 707-712.

[29] R. Herbert, M. Christl, *Chem. Ber.* **1979**, *112*, 2012-2021.

[30] a) G. E. Herberich, Chapter 5: Boron Rings Ligated to Metals, in *Comprehensive Organometallic Chemistry II*, ed. E. W. Abel, F. G. A. Stone and G. Wilkinson, Pergamon Press, Oxford, 1995; vol. 1, pp. 197; b) B. Su, R. Kinjo, *Synthesis* **2017**, *49*, 2985-3034.

[31] a) J. S. Rogers, X. Bu, G. C. Bazan, *J. Am. Chem. Soc.* **2000**, *122*, 730-731; b) H. Braunschweig, S. Demeshko, W. C. Ewing, I. Krummenacher, B. B. Macha, J. D. Mattock, F. Meyer, J. Mies, M. Schafer, A. Vargas, *Angew. Chem. Int. Ed.* **2016**, *55*, 7708–7711; c) J. Böhnke, H. Braunschweig, J. O. C. Jimén-Halla, I. Krummenacher, T. E. Stennett, *J. Am. Chem. Soc.* **2018**, *140*, 848–853.

[32] W. Siebert, *J. Organomet. Chem.* **2009**, *694*, 1718–1722; b) P. Braunstein, U. Englert, G. E. Herberich, M. Neuschütz, M. U. Schmidt, *J. Chem. Soc. Dalton Trans.* **1999**, 2807–2812.

[33] a) J. R. Bowser, A. Bonny, J. R. Pipal, R. N. Grimes, *J. Am. Chem. Soc.* **1979**, *101*, 6229–6236; b) J. R. Pipal, R. N. Grimes, *Inorg. Chem.* **1979**, *18*, 257–263; c) K. Geetharani, S. K. Bose, S. Sahoo, S. Ghosh, *Angew. Chem. Int. Ed.* **2011**, *50*, 3908 –3911.

[34] a) V. R. Miller, R. Weiss, R. N. Grimes, *J. Am. Chem. Soc.* **1977**, *99*, 5646-5651; b) K. Kawamura, M. Shang, O. Wiest, T. P. Fehlner, *Inorg. Chem.* **1998***, 37, 608−609.*

[35] U. Kolle, F. Khouzami, B. Fuss, *Angew. Chem. Int. Ed.* **1982**, *21*, 131-132.

[36] D. Sharmila, R. Ramalakshmi, K. K. V. Chakrahari, B. Varghese, S. Ghosh, *Dalton Trans.* **2014**, *43*, 9976-9985.

[37] Compound **4** was synthesised by Morley's group in the year of 1991. To the best of our knowledge, the X-ray structure of this compound is not reported.

[38] Gaussian 09, Revision D.01, M. J. Frisch, G. W. Trucks, H. B. Schlegel, G. E. Scuseria, M. A. Robb, J. R. Cheeseman, G. Scalmani, V. Barone, B. Mennucci, G. A. Petersson, H. Nakatsuji, M. Caricato, X. Li, H. P. Hratchian, A. F. Izmaylov, J. Bloino, G. Zheng, J. L. Sonnenberg, M. Hada, M. Ehara, K. Toyota, R. Fukuda, J. Hasegawa, M. Ishida, T. Nakajima, Y. Honda, O. Kitao, H. Nakai, T. Vreven, J. A. Montgomery, Jr., J. E. Peralta, F. Ogliaro, M. Bearpark, J. J. Heyd, E. Brothers, K. N. Kudin, V. N. Staroverov, T. Keith, R. Kobayashi, J. Normand, K. Raghavachari, A. Rendell, J. C. Burant, S. S. Iyengar, J. Tomasi, M. Cossi, N. Rega, J. M. Millam, M. Klene, J. E. Knox, J. B. Cross, V. Bakken, C. Adamo, J. Jaramillo, R. Gomperts, R. E. Stratmann, O. Yazyev, A. J. Austin, R. Cammi,

C. Pomelli, J. W. Ochterski, R. L. Martin, K. Morokuma, V. G. Zakrzewski, G. A. Voth, P. Salvador, J. J. Dannenberg, S. Dapprich, A. D. Daniels, O. Farkas, J. B. Foresman, J. V. Ortiz, J. Cioslowski, and D. J. Fox, Gaussian, Inc. Wallingford CT, 2013.

[39] Y. Zhao and D. G. Truhlar, *Theor. Chem. Acc.* **2008**,*120*, 215–241.

[40] a) F. Weigend and R. Ahlrichs, *Phys. Chem. Chem. Phys.* **2005**, *7*, 3297-3305. b) F. Weigend, *Phys. Chem. Chem. Phys.* **2006**, *8*, 1057-1065.

[41] a) E. D. Glendening, A. E. Reed, J. E. Carpenter, F. Weinhold, NBO Program 3.1, W. T. Madison: 1988. b) A. E. Reed, F. Weinhold, L. A. Curtiss, *Chem. Rev.* **1988**, *88*, 899-926.

[42] S. Grimme, J. Antony, S. Ehrlich, H. Krieg, *J. Chem. Phys .***2010**, *132*, 154104–154119.

[43] a) G. M. Sheldrick, *Acta Cryst.* **2015**, *A71,* 3–8; b) G. M. Sheldrick, SHELXS97 and SHELXL97. Program for Crystal Structure Solution and Refinement,University of Gottingen: Germany, 1997.

[44] G. M. Sheldric, *Acta Cryst.* **2015**, *C71*, 3–8.

[45] O. V. Dolomanov, L. J. Bourhis, R. J. Gildea, J. A. K. Howard, H. Puschmann, *J. Appl. Cryst.* **2009**, *42*, 339–341.

Entry for the Table of Contents

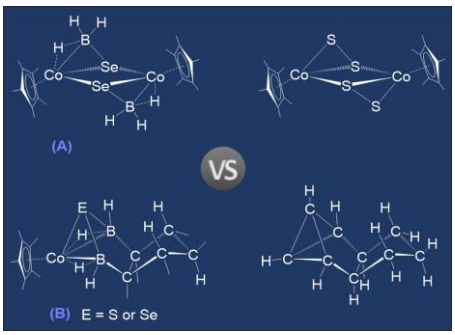

Chalcogen stabilized *bis*-hydridoborate complexes of cobalt with unusual bonding have been synthesized. Complexes **(A)** and **(B)** are the structural mimic of species $[(Cp^*Co)_2(\mu\text{-}S)_2(\kappa\text{-}S)_2]$ and tetracyclo[4.3.0.0^{2,4}.0^{3,5}]nonane respectively (see picture)